Single-waveguide dual-wavelength interband cascade lasers

Lu Li,[1,a)] Lihua Zhao,[1] Yuchao Jiang,[1] Rui Q. Yang,[1,a)] Joel C. Keay,[2] Tetsuya D. Mishima,[2] Michael B. Santos,[2] and Matthew B. Johnson[2]
[1]*School of Electrical and Computer Engineering, University of Oklahoma, Norman, Oklahoma 73019, USA*
[2]*Homer L. Dodge Department of Physics and Astronomy, University of Oklahoma, Norman, Oklahoma 73019, USA*

(Received 29 August 2012; accepted 16 October 2012; published online 26 October 2012)

Dual-wavelength interband cascade (IC) lasers with two different cascade regions in a single waveguide have been demonstrated in pulsed conditions to simultaneously lase based on spatially overlapping fundamental vertical modes near 5 and 6 μm. The fabricated broad-area devices operate at temperatures up to 155 K and 235 K in cw and pulsed modes, respectively. The temperature dependence of the device performance characteristics has been investigated. The threshold current of the dual wavelength IC lasers at the shorter wavelength showed different characteristics from that at the longer wavelength. © *2012 American Institute of Physics*. [http://dx.doi.org/10.1063/1.4764910]

Semiconductor lasers that are capable of emitting at two or more distinct wavelengths have been pursued[1–8] for applications such as optical communications, optical recording systems, spectroscopy, and nonlinear optics. It is especially desirable to achieve two different lasing wavelengths from a single waveguide configuration for intra-cavity nonlinear optics and good beam quality with less divergence.[3,4] For interband diode lasers, however, it is difficult to simultaneously lase at two distinct wavelengths from a single waveguide, because of the preferential recombination of carriers in the active region where the lasing is first achieved, and the absorption loss of the shorter wavelength (SW) light by the longer wavelength (LW) active region. This preferential recombination issue can be circumvented by using a heavily doped Esaki tunneling junction[2–4] so that uniform injection of carriers into the separate active regions is ensured by their series connection. Unfortunately, the heavily doped Esaki tunneling junction also introduces significant absorption loss. To minimize such a loss, active regions for different wavelengths are separated by a substantial distance and the waveguide is designed for lasing based on higher-order vertical modes instead of the fundamental mode, which also has the disadvantageous effect of making the laser beam more divergent.[3,4]

The above mentioned issue can be avoided in optically pumped interband lasers by dividing the waveguide with a thin barrier layer that is transparent to the pump beam,[5] and in quantum cascade (QC) lasers[6–8] based on intersubband transitions, where the gain spectrum is narrow and the active regions are connected in series. Alternatively, interband cascade (IC) lasers,[9] which utilize the broken-gap alignment in type-II quantum wells to form cascade stages, should in principle be more promising than conventional interband diode lasers in achieving simultaneous lasing at two (or more) wavelengths from two different cascade regions that are adjacent to each other within a single waveguide. By eliminating the use of heavily doped Esaki tunneling junctions and keeping the interband transition, it is possible for IC lasers to achieve dual-wavelength lasing with a single-waveguide and with a good beam quality and a low threshold current. Previously, a dual-wavelength IC laser was demonstrated with two separate waveguides[10] rather than a single waveguide. Hence, the promise of dual-wavelength interband diode lasers based on the fundamental mode with good single-beam quality for academic interest and certain applications has remained unfulfilled. In this paper, we report our demonstration of single waveguide dual-wavelength IC lasers that simultaneously lase in pulsed mode near 5 and 6 μm. With clear evidence through detailed characterization, we show that the simultaneous lasing at two wavelengths is indeed from two different cascade regions within the same waveguide.

The dual-wavelength IC laser structure was designed with two different cascade regions stacked on top of one another. The bottom cascade region consists of 12 identical stages for lasing at the LW, near 6 μm (Ref. 11) and the top cascade region is composed of 9 stages for lasing at the SW, near 5 μm.[12] IC lasers with the same cascade stages corresponding to these two individual wavelengths were reported earlier.[11,12] It should be noted that the electron injectors were doped at a relatively low level ($\sim 1 \times 10^{17}$ cm^{-3}) compared to the high doping used in recently introduced re-balanced IC lasers.[13] The laser structure was grown on an n^+-doped InAs substrate in an Intevac GEN II molecular beam epitaxy (MBE) system. In addition to the cascade regions, the IC laser structure also comprises a 1.8 μm-thick n^{++}-type InAs bottom cladding layer (Si doped to 5×10^{18} cm^{-3}), a 1.1 μm-thick undoped InAs bottom separate confinement layer (SCL), a 1.35 μm-thick undoped InAs top SCL, and a 35-nm-thick n^{++}-type InAs top contact layer, as shown in inset to Fig. 1. For this single waveguide, the calculated fundamental modes at both the longer and shorter wavelengths as shown in Fig. 1 suggest that their vertical optical field profiles essentially overlap, which should result in a desirable single beam with good quality.

Lasers were processed into deep-etched 150 μm-wide broad-area mesa stripe lasers by contact photolithography

[a)]Authors to whom correspondence should be addressed. Electronic addresses: lilu@ou.edu and rui.q.yang@ou.edu.

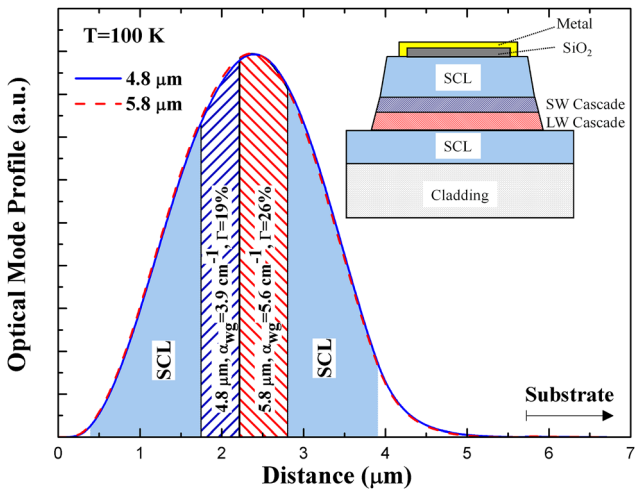

FIG. 1. Schematic layer structure and simulated optical mode profile of the dual-wavelength IC lasers at 100 K. The optical waveguide loss α_{wg} is estimated mainly from the cladding layer and top metal contact without including the absorption loss in the cascade region.

and wet chemical etching. A 200-nm-thick and 90 μm-wide SiO_2 insulating layer was deposited on the center of the mesa stripe and plays a role in the optical cladding. The current injection is provided through two sides of a 100 μm-wide and 150-nm-thick Ti/Au layer on the top center of the mesa, as shown in Fig. 1. This current injection configuration through two side metal contacts should reduce the optical loss from metal as discussed in Ref. 12. The wafer was cleaved into laser bars about 1 mm long, and the facets were left uncoated. The laser bars were mounted epilayer side up on copper heat sinks with indium solder and placed on the cold finger of a cryostat for measurements in continuous wave (cw) and pulsed modes. In pulsed measurements, the applied current pulse width is 1μs at a repetition rate of 10 kHz (lasing spectra) and 1 kHz (current-light curves).

These broad-area devices lase in cw mode with a maximum operating temperature of 155 K at 6.12 μm. The lowest threshold current density was 4.7 A/cm^2 and 2.1 A/cm^2 in cw and pulsed modes, respectively, for a 1.1-mm-long device at 80 K. Figure 2 shows the measured current-voltage-light (*I-V-L*) characteristics of a 0.92-mm-long device. The threshold current density of this device was 6.5 A/cm^2 at 80 K with a threshold voltage of 5.33 V. The output power was 55 mW/facet at 300 mA. The lasing wavelength (inset to Fig. 2) near the threshold showed a red shift from 5.78 μm at 80 K to 6.06 μm at 150 K, in good agreement with the earlier observations for lasers with the corresponding homogenous cascade stages for lasing near 6 μm.[11] We also examined cw lasing spectra at various current levels above the threshold and found no substantial change of the lasing wavelength except the usual broadening of spectra with increasing current. These results indicate that only the longer wavelength cascade region contributed to the above cw lasing, while the shorter wavelength cascade region contributed to the relatively high threshold voltage observed.

In pulsed operation, the device was able to lase at temperatures up to 235 K and had a low threshold current density (3.5 A/cm^2) at 80 K. The output power of the laser continued to increase with current and did not show any saturation up to the current limit of the pulsed current source (3 A) (see Fig. 3 for currents up to 1 A). (The current reading from the current source was not accurate for currents greater than 1 A, because of impedance mismatch and consequent pulse ringing. Nevertheless, this does not affect our explanations and conclusion for this work.) As observed from the near threshold pulsed lasing spectra (inset to Fig. 3), when the temperature is 220 K and above, the lasing peak hopped from the longer wavelength (near 6.2 μm) to the shorter wavelength (near 5.2 μm). The shorter lasing wavelength is in good agreement with the wavelength for lasers with the corresponding homogenous cascade stages for lasing near 5.2 μm.[12] This indicates that lasing was achieved from the SW cascade region and could be realized simultaneously with that of the LW region at temperatures below 220 K for certain current levels. Indeed, pulsed lasing was observed simultaneously at the two design wavelengths for all the devices that were tested. Figure 4 shows how the lasing spectrum of a device at 160 K evolved from single- to dual-wavelength emission with an increase of pulsed current. In Fig. 4, a logarithmic scale is used for the 1.7 and 2.0 A

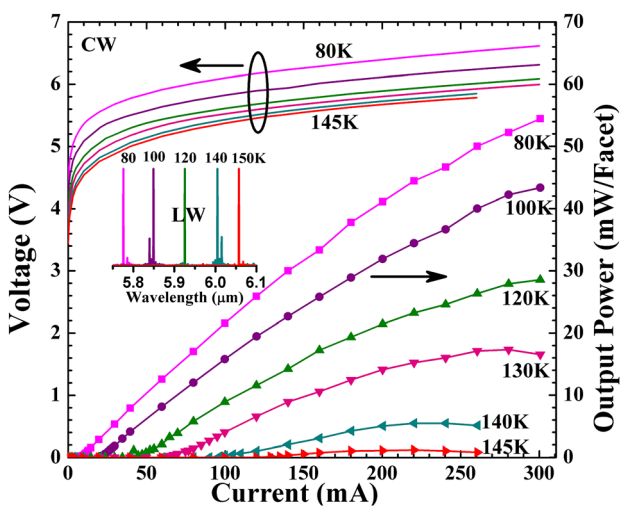

FIG. 2. Current-voltage-light characteristics of a 0.92-mm-long device in cw mode at various heat-sink temperatures. The inset shows the lasing spectra at several temperatures.

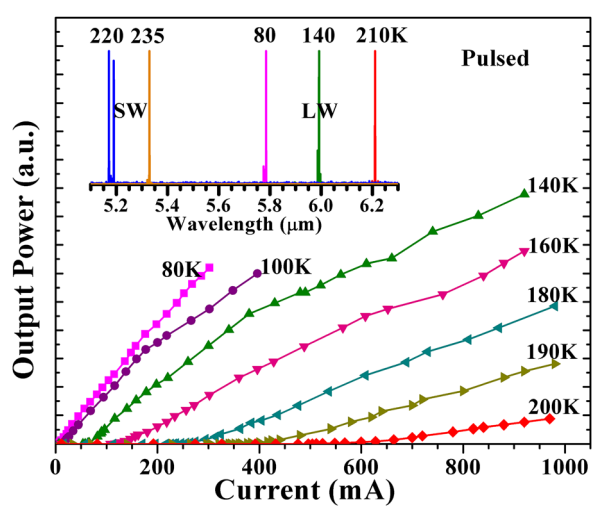

FIG. 3. Current-light characteristics and lasing spectra of a 0.92-mm-long device in pulsed modes at various heat-sink temperatures. The inset shows lasing spectra at several temperatures.

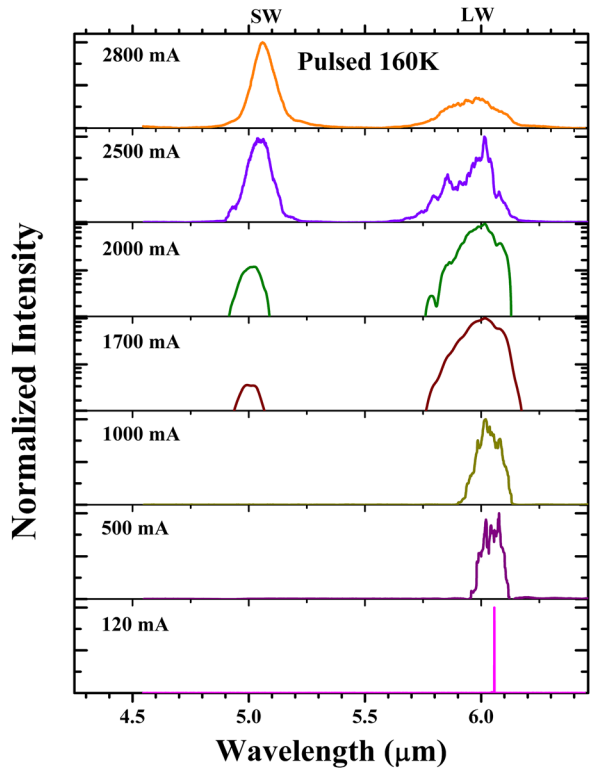

FIG. 4. Emission spectra of the 0.92-mm-long device at 160 K under current pulses at several levels. The spectra are shifted vertically for clarity, and a logarithmic scale is used at 2000 and 1700 mA.

spectra because the lasing intensity at the shorter wavelength is initially much weaker than that at the longer wavelength. As shown in Fig. 4, the device first lased at a single wavelength of 6.06 μm near the threshold (120 mA). With an increase of the current, the spectrum became wide around 6 μm, and then the second lasing peak at the shorter wavelength near 5 μm appeared at 1.7 A. When the current was increased further, the emission intensity at the shorter wavelength was enhanced significantly, at 2.5 A became comparable to that at the longer wavelength, and at 2.8 A the light intensity at the shorter wavelength exceeded that at the longer wavelength. Far-field in the vertical direction was measured at all current levels, and exhibited a stable single-lobe pattern peaked at the direction normal to the facet. This confirmed that the lasing was based on the spatially overlapping fundamental vertical modes at two wavelengths.

Similar spectral characteristics of dual wavelength operation were observed from 100 to 210 K. Lasing at the shorter wavelength began at a higher current, I_{thsw}, compared to the threshold current, I_{th}, at the longer wavelength. Above 210 K, lasing occurred only at the shorter wavelength. The peak wavelength's dependence on temperature for several currents in cw and pulsed modes is shown in Fig. 5. The solid and open circles are the measurement results for cw and pulsed modes, respectively, near their threshold currents (I_{th}) with their corresponding fitted lines giving temperature tuning rates of 3.97 nm/K and 3.23 nm/K, respectively. The peak wavelength at the shorter wavelength near I_{thsw} (open triangles) had a temperature tuning rate of 3.16 nm/K, which is approximately the same as that for the longer wavelength near I_{th} in pulsed mode. At 2.5 A, the peak wavelength shifted with temperature at a rate

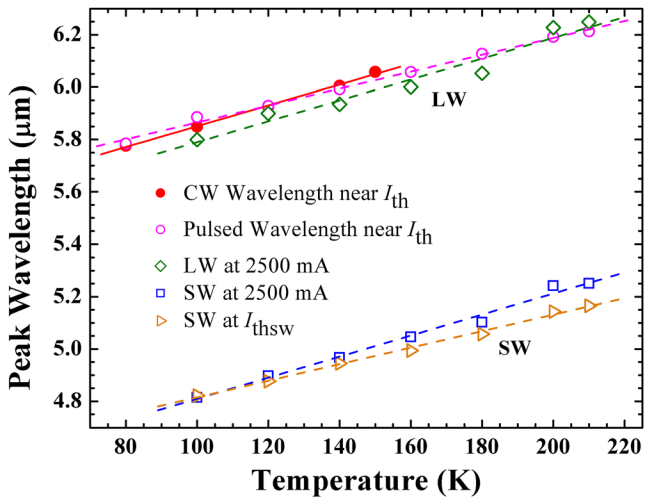

FIG. 5. Temperature dependence of peak wavelengths for the 0.92-mm-long device at various current levels.

4.03 nm/K for the SW sector and 3.98 nm/K for the LW sector. These results suggest that there is no interference of lasing wavelength from different sectors, and the LW lasing is from the bottom 12-cascade region, while the SW lasing is from the top 9-cascade region.

It is interesting to observe that the threshold current for the shorter wavelength (I_{thsw}) has an unusual temperature dependence and is much higher at low temperatures compared to the threshold for the longer wavelength (I_{th}), as shown in Fig. 6. Based on our simulations, the confinement factor Γ is larger for the LW sector with the bottom 12-stage cascade region, while the waveguide loss α_{wg} from the cladding layer and metal contact is smaller for the SW sector as shown in Fig. 1. Combining these two factors at low temperatures, the required threshold gain is about the same for the LW and SW sectors. However, because the band-gap of the LW cascade region is smaller than the photon energy emitted from the SW cascade region, the SW light generated from the top cascade region can be absorbed in the LW cascade region, resulting in an extra high absorption loss α_{sw} at the shorter wavelength. Thus, it is not surprising that the threshold current I_{thsw} for lasing at the shorter wavelength is much higher than I_{th} for lasing at the longer wavelength at low temperatures.

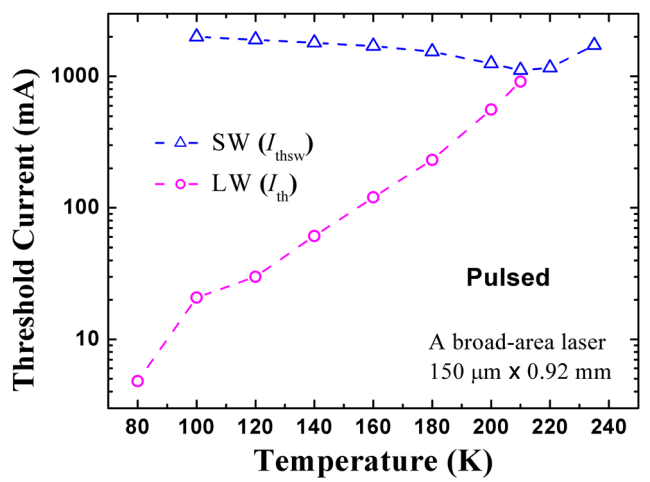

FIG. 6. Threshold current for lasing at the longer and shorter wavelengths at different heat-sink temperatures.

When the temperature is raised, the emission wavelength from both cascade regions becomes longer with reduced gain coefficient[14] and increased waveguide loss α_{wg} from the metal/cladding layers, although the increase of α_{wg} is slower for the shorter wavelength. Consequently, one would expect an increase of threshold current with temperature for both wavelengths if the absorption loss α_{sw} from the cascade region did not change. However, only the threshold current for the longer wavelength, I_{th}, increased with the temperature, while the threshold current for the shorter wavelength, I_{thsw}, decreased with the temperature. This suggests that the absorption loss α_{sw} at the SW from the cascade region was reduced with the temperature at a rate significantly faster than the combined effects of the increase of α_{wg} and the reduction of the gain coefficient. Above 210 K, lasing was achieved only at the shorter wavelength, and the threshold current increased with the temperature as the conventional mechanisms dominated.

In summary, dual-wavelength IC lasers with a single waveguide have been demonstrated in pulsed conditions with simultaneous lasing based on essentially overlapping fundamental vertical modes at two distinct wavelengths near 5 and 6 μm. Unusual temperature dependences of the laser characteristics were observed. Based on the flexibility associated with IC lasers in manipulating the number of cascade stages for different wavelengths and possible improvements in design and device fabrication, dual-wavelength or even multiple-wavelength IC lasers with enhanced device performance such as low threshold current and cw operation are expected to be developed in the future.

This work was supported by the National Science Foundation (ECCS-1002202) and by C-SPIN, the Oklahoma/Arkansas MRSEC (DMR-0520550).

[1]K. J. Beernink, R. L. Thornton, and H. F. Chung, Appl. Phys. Lett. **64**, 1082 (1994).
[2]J. C. Garcia, E. Rosencher, P. Collot, N. Laurent, J. L. Guyaux, B. Vinter, and J. Nagle, Appl. Phys. Lett. **71**, 3752 (1997).
[3]J. Yan, J. Cai, G. Ru, X. Yu, J. Fan, and F.-S. Choa, IEEE Photon. Technol. Lett. **18**, 1777 (2006).
[4]S. M. Nekorkin, A. A. Biryukov, P. B. Demina, N. N. Semenov, B. N. Zvonkov, V. Ya. Aleshkin, A. A. Dubinov, V. I. Gavrilenko, K. V. Maremyanin, S. V. Morozov *et al.*, Appl. Phys. Lett. **90**, 171106 (2007).
[5]R. Kaspi, A. P. Ongstad, G. C. Dente, M. L. Tilton, and A. Tauke-Pedretti, IEEE Photon. Technol. Lett. **20**, 1467 (2008).
[6]A. Tredicucci, C. Gmachl, F. Capasso, D. L. Sivco, A. L. Hutchinson, and A. Y. Cho, "A multiwavelength semiconductor laser," Nature **396**, 350 (1998).
[7]C. Gmachl, D. L. Sivco, J. N. Baillargeon, A. L. Hutchinson, F. Capasso, and A. Y. Cho, Appl. Phys. Lett. **79**, 572 (2001).
[8]F. Toor, S. S. Howard, D. L. Sivco, and C. F. Gmachl, IEEE J Quantum Electron. **45**, 914 (2009).
[9]R. Q. Yang, "Infrared laser based on intersubband transitions in quantum wells," Superlattices Microstruct. **17**, 77 (1995).
[10]K. Mansour, C. J. Hill, Y. Qiu, and R. Q. Yang, in *The Conf. on Lasers and Electro-Optics (CLEO) and the Quantum Electronics and Laser Science Conf. (QELS)* (2008), paper CTuZ4.
[11]L. Li, Z. Tian, Y. Jiang, H. Ye, R. Q. Yang, T. D. Mishima, M. B. Santos, and M. B. Johnson, in *The Conf. on Lasers and Electro-Optics (CLEO) and the Quantum Electronics and Laser Science Conf. (QELS)* (2012), paper CF3K.2.
[12]Z. Tian, Y. Jiang, L. Li, R. T. Hinkey, Z. Yin, R. Q. Yang, T. D. Mishima, M. B. Santos, and M. B. Johnson, IEEE J. Quantum Electron. **48**, 915 (2012).
[13]I. Vurgaftman, W. W. Bewley, C. L. Canedy, C. S. Kim, M. Kim, C. D. Merritt, J. Abell, J. R. Lindle, and J. R. Meyer, Nat. Commun. **2**, 585 (2011).
[14]Y.-M. Mu and R. Q. Yang, J. App. Phys. **84**, 5357 (1998).